AD-A105 594 SYDNEY UNIV (AUSTRALIA) COASTAL STUDIES UNIT F/G 14/2
CALIBRATION AND DATA CORRECTION PROCEDURES FOR FLOW METERS AND --ETC(U)
JUL 81 P NIELSEN, P J COWELL N00014-80-G-0001
UNCLASSIFIED CSU-TR-81/1 NL

1 OF 1
AD A
105594

END
DATE
FILMED
11-81
DTIC

END
DATE
FILMED
11-81
DTIC

SECURITY CLASSIFICATION OF THIS PAGE (When Data Entered)

REPORT DOCUMENTATION PAGE		READ INSTRUCTIONS BEFORE COMPLETING FORM
1. REPORT NUMBER	2. GOVT ACCESSION NO. AD-A105594	3. RECIPIENT'S CATALOG NUMBER
4. TITLE (and Subtitle) CALIBRATION AND DATA CORRECTION PROCEDURES FOR FLOW METERS AND PRESSURE TRANSDUCERS COMMONLY USED BY THE COASTAL STUDIES UNIT. C.S.U. TECH. REP. 81/1		5. TYPE OF REPORT & PERIOD COVERED
		6. PERFORMING ORG. REPORT NUMBER
7. AUTHOR(s) P. NIELSEN & P.J. COWELL		8. CONTRACT OR GRANT NUMBER(s) Grant N-00014-80-G-0001
9. PERFORMING ORGANIZATION NAME AND ADDRESS Coastal Studies Unit, Dept. of Geography University of Sydney Sydney. N.S.W. 2006 Australia		10. PROGRAM ELEMENT, PROJECT, TASK AREA & WORK UNIT NUMBERS NR 388-157
11. CONTROLLING OFFICE NAME AND ADDRESS ONR, Coastal Sciences Program Code 462 Arlington, VA 22217		12. REPORT DATE
		13. NUMBER OF PAGES
14. MONITORING AGENCY NAME & ADDRESS (if different from Controlling Office)		15. SECURITY CLASS. (of this report) Unclassified
		15a. DECLASSIFICATION/DOWNGRADING SCHEDULE

16. DISTRIBUTION STATEMENT (of this Report)

Distribution of this document is unlimited

Approved for public release; Distribution Unlimited

17. DISTRIBUTION STATEMENT (of the abstract entered in Block 20, if different from Report)

18. SUPPLEMENTARY NOTES

19. KEY WORDS (Continue on reverse side if necessary and identify by block number)

20. ABSTRACT (Continue on reverse side if necessary and identify by block number)

This report describes calibration procedures and results for two types of instruments commonly used by the Coastal Studies Unit: a bidirectional ducted flow meter and a strain gage pressure transducer. These instruments each constitute a system comprising a sensor head which issues a pulsating signal and a control box which electronically integrates the pulses into an analogue voltage which is then recorded. It is the response characteristics of these systems as a whole that are examined herein.

DD FORM 1 JAN 73 1473 EDITION OF 1 NOV 65 IS OBSOLETE

S/N 0102-LF-014-6601

Unclassified

SECURITY CLASSIFICATION OF THIS PAGE (When Data Entered)

412520

There are two models of the flow meter system: 'Version 1' and 'Version 2'. Whilst Version 2 is generally considered in this report, the distinguishing response characteristics of Version 1 are described on page 19.

In addition to the calibrations, data analysis correction procedures and limitations are also described in this report.

Both the flow meter and transducer systems have been physically described along with their use, and place in the general data acquisition system, by Bradshaw et al. (1979; attached for reference as an appendix).

INTRODUCTION

This report describes calibration procedures and results for two types of instruments commonly used by the Coastal Studies Unit: a bidirectional ducted flow meter and a strain gage pressure transducer. These instruments each constitute a system comprising a sensor head which issues a pulsating signal, and a control box which electronically integrates the pulses into an analogue voltage which is then recorded. It is the response characteristics of these systems as a whole that are examined herein.

There are two models of the flow meter system: 'Version 1' and 'Version 2'. Whilst Version 2 is generally considered in this report, the distinguishing response characteristics of Version 1 are described on page 19.

In addition to the calibrations, data analysis correction procedures and limitations are also described in this report.

Both the flow meter and transducer systems have been physically described along with their use, and place in the general data acquisition system, by Bradshaw et al. (1979; attached for reference as an appendix).

CONTENTS

ILLUSTRATIONS

SECTION 1

CALIBRATION OF DUCTED IMPELLER FLOWMETERS

Abstract

The purpose of the experiments described below has been to calibrate the Coast-- Studies Unit's ducted impeller flowmeters.

Tests were carried out for linearity, frequency response, and the effect of the flow meter being placed at an angle to the flow.

Methods for correction of spectra and time series are devised.

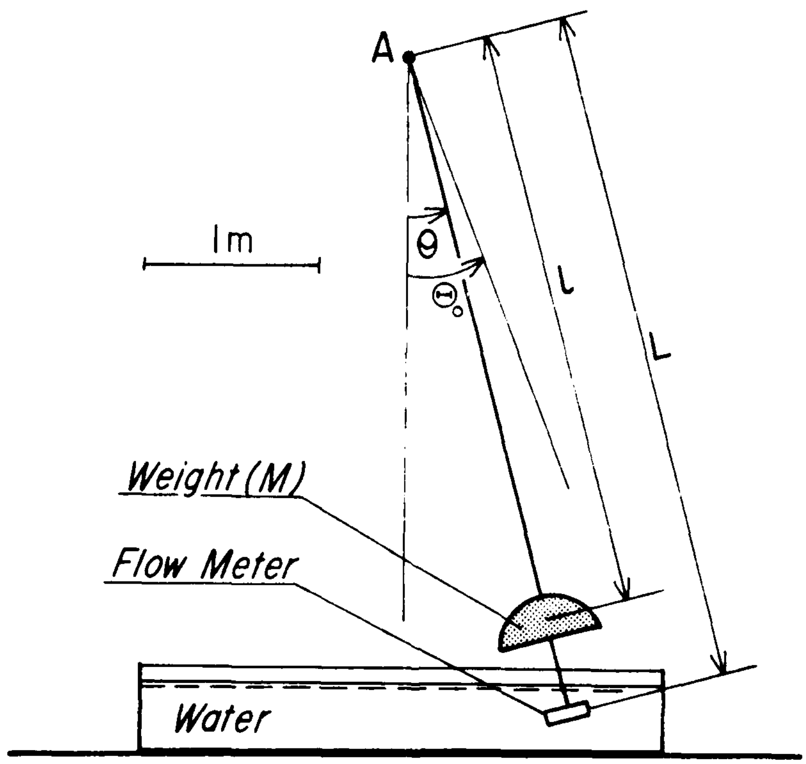

Figure 1: Experimental setup. The pendulum was started from rest in the position $\Theta = \Theta_0$ at $t = 0$. Instantaneous values of Θ were measured by a potentiometer at A, and instantaneous flow meter velocities were then derived from $u(t) = L \frac{d\Theta}{dt}$.

Experimental setup

The flowmeters, placed at the end of a big pendulum moved through still water.

The instantaneous angle Θ was measured by a potentiometer attached to the pendulum and its axle.

The pendulum consisted of a 50 kg weight suspended on a ½ inch water pipe. The period of oscillation could be changed by moving the weight along the pipe or by changing the length of the pipe. In this way periods between 2.5 and 5.5 seconds were obtained.

The lateral stability of the pendulum did not cause problems. Neither did flexing of the pipe. Waves in the water tub were always of negligible height (less than 2 cm), and in general the water velocities that were made visible by impurities were negligible compared to the pendulum motion.

Determination of $\Theta(t)$

The relation between the output voltage P of the potentiometer and the angle Θ was tested over the total range of Θ. The goodness of fit parameter for linearity was

$$r = .99991$$

so Θ can be regarded as a linear function of P.

The amplitude $\Theta(t_m)$ related to an extreme voltage $P(t_m)$ can then be calculated when the starting angle Θ_0, the starting voltage P_o and the voltage $\bar{P}$ related to $\Theta = 0$ are known

$$\Theta = \frac{P_m - \bar{P}}{P_o - \bar{P}} \Theta_0 \qquad (1)$$

The Motion of the Pendulum

For the velocities considered ($\sim$ 1 m/s) and the actual dimensions of the flowmeter ($\sim$ 5 cm) one would expect the flow around the flowmeter to be turbulent so that the notation of figure 1 the motion would be given by:

$$Ml\,\frac{d^2\Theta}{dt^2} \;+\; K\left|L\frac{d\Theta}{dt}\right|L\frac{d\Theta}{dt} \;+\; Mg\Theta \;=\; 0 \qquad (2)$$

with the drag coefficient K being nearly independent of the flow speed $L\frac{d\Theta}{dt}$.

This equation, which is itself only an approximation ($\sin\Theta \simeq \Theta$ and $K \simeq$ const), cannot be solved analytically. Instead we assume that the motion has the form

$$\Theta(t) \;=\; \boldsymbol{\Theta}(t)\;\cos\omega t \qquad (3)$$

where $\boldsymbol{\Theta}(t)$ is the instantaneous amplitude (in radians) of the pendulum. In the following we assume that $\boldsymbol{\Theta}(t)$ varies slowly, or more precisely

$$\frac{d\boldsymbol{\Theta}}{dt} \;<<\; \omega\boldsymbol{\Theta} \qquad (4)$$

so that

$$\frac{d\Theta}{dt} \;=\; \frac{d}{dt}\,(\boldsymbol{\Theta}\cos\omega t) \;\simeq\; -\,\omega\boldsymbol{\Theta}\sin\omega t \qquad (5)$$

The period of the oscillation and thus ω appeared to be independent of $\boldsymbol{\Theta}$, within the experimental accuracy.

With $\frac{d\Theta}{dt}$ given by (5) the total energy of the pendulum is:

$$E(t) \;=\; \tfrac{1}{2}M(l\omega\boldsymbol{\Theta})^2 \qquad (6)$$

and thus

$$\frac{dE}{dt} \;=\; Ml^2\omega^2\boldsymbol{\Theta}\,\frac{d\boldsymbol{\Theta}}{dt} \;\propto\; \boldsymbol{\Theta}\,\frac{d\boldsymbol{\Theta}}{dt} \qquad (7)$$

where "$\propto$" means proportional to.

The drag force has the form

$$F_D \propto \Theta^2 |\sin \omega t| \sin \omega t \tag{8}$$

see (2) and (5). And thus the energy dissipation rate (velocity times drag) is:

$$\frac{dE}{dt} \propto - \Theta^3 |\sin \omega t| \sin^2 \omega t \tag{9}$$

and the average over half a period is

$$\overline{\frac{dE}{dt}} \propto - \Theta^3 \tag{10}$$

From (7) and (10) we then get a differential equation for the decay of Θ,

$$\Theta \frac{d\Theta}{dt} = - \alpha \Theta^3 \tag{11}$$

where α is a constant.

By separation of the variables we get

$$- \frac{d\Theta}{\Theta^2} = \alpha dt \tag{12}$$

and thus

$$\frac{1}{\Theta} = \alpha t + \text{const} \tag{13}$$

From the starting conditions $\Theta(o) = \Theta_o$ we find the integration constant and the final expression is:

$$\frac{1}{\Theta} = \frac{1}{\Theta_o} + \alpha t \tag{14}$$

The flow velocity through the flow meter is approximately

$$u = L\omega\Theta \sin \omega t \tag{15}$$

so for the decay of its amplitude U we get

$$\frac{1}{U} = \frac{1}{L\omega\Theta_o} + \beta t \tag{16}$$

The relation (16) can only be expected to hold when the drag coefficient K is a constant, that is for fully developed turbulent flow. When this condition is not fulfilled, the measured values of u cannot be fitted perfectly by (16). However the discrepancy is easily overcome by adding a small second order term

$$\frac{1}{U} = \frac{1}{L\omega\Theta_o} + \beta t + \beta_2 t^2 \tag{17}$$

see figure 9.

Frequency Response

The output, v of the flow meter for a given periodic input U sin ωt may be written as

$$v(t) = G\, U \sin \omega(t-\delta) \tag{18}$$

Where G is the gain or amplitude reduction and δ is the time lag.

In general G and δ may depend on both ω and U. However the measurements show that the variation with U is small, see figures 3 and 4. That is, the instruments are linear.

Figure 2 shows how the time lag δ is determined from the interval between a θ-zero-crossing and the following v-zero-crossing.

The gain was found from the peak values V of v(t) by comparing to simultaneous values of $U = L\omega\Theta$.

$$G = \frac{V(t)}{U(t)} \tag{19}$$

U(t) being determined from (16) or (17).

Each run gave 20-35 values of G and δ, depending on the damping rate.

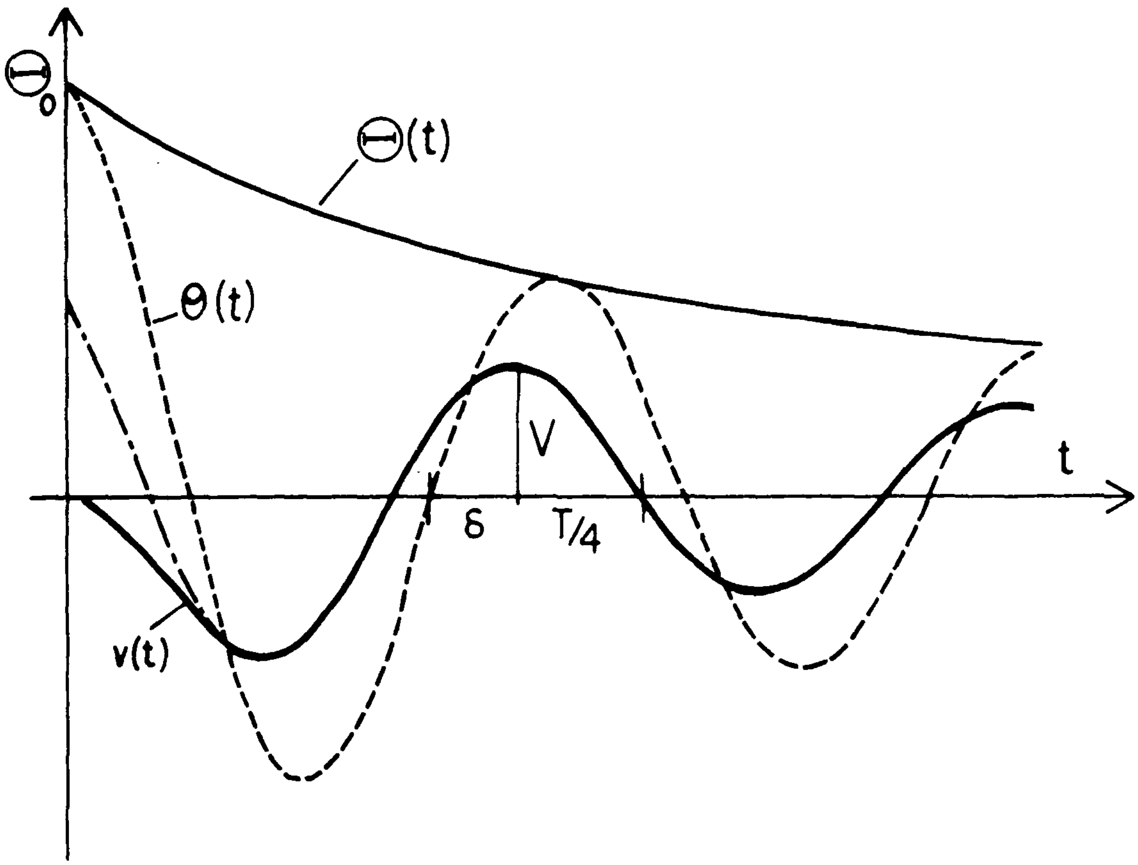

Figure 2: Idealised time series $\theta(t)$, $\Theta(t)$ and $v(t)$. The real velocity is $u(t) = L\frac{d\theta}{dt} \simeq L\omega\Theta \sin \omega t$.

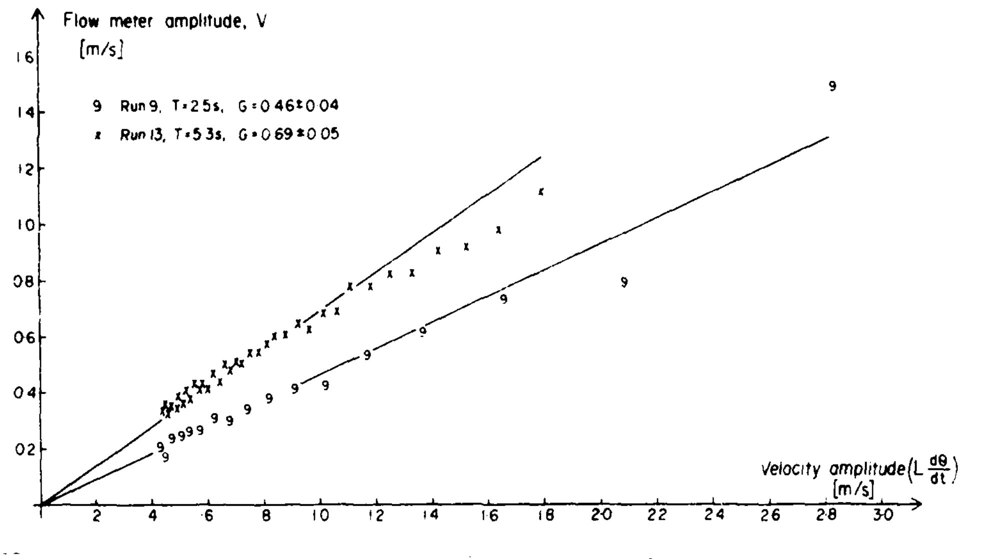

Figure 3: Comparison between real velocities and flow meter output. The instrument appears to be practically linear.

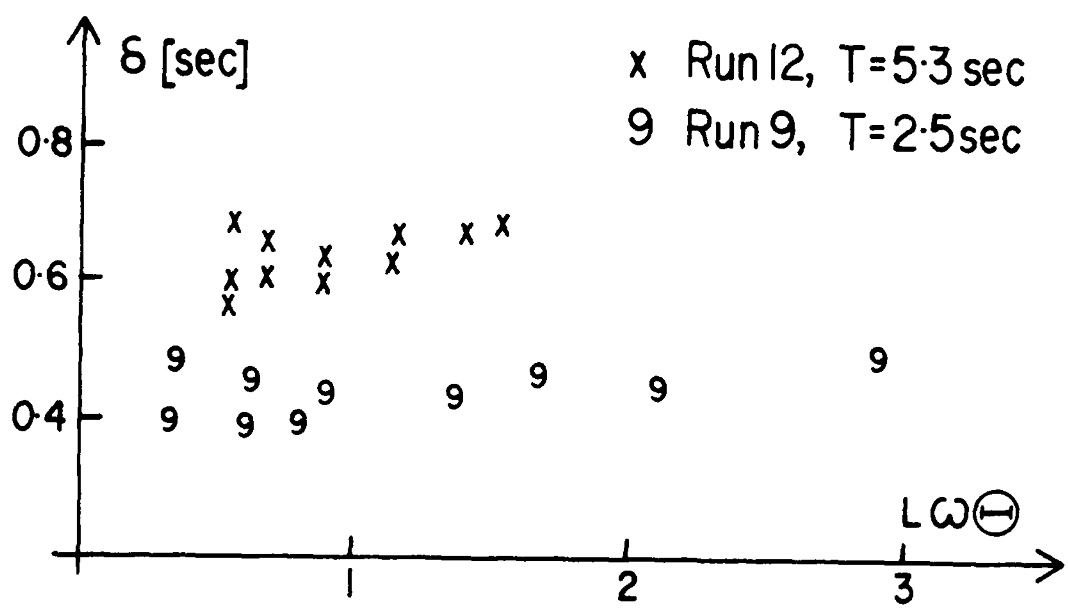

Figure 4: Time lag versus velocity amplitude. δ is practically independent of the velocity amplitude.

The obtained values of G and the phase lag $\phi = \frac{\delta}{T} 360^{o}$ are shown in figures 5 and 6.

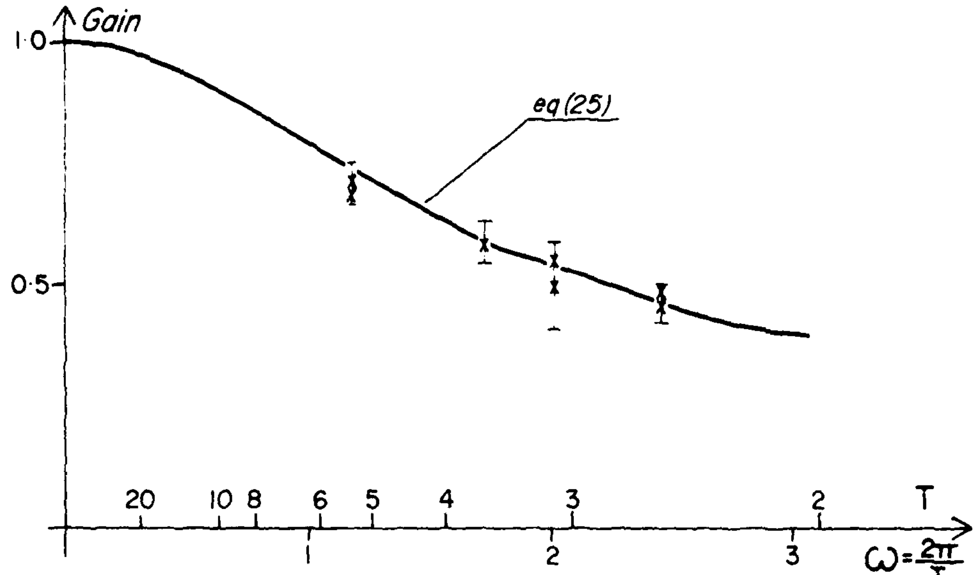

Figure 5: Gain as function of ω.

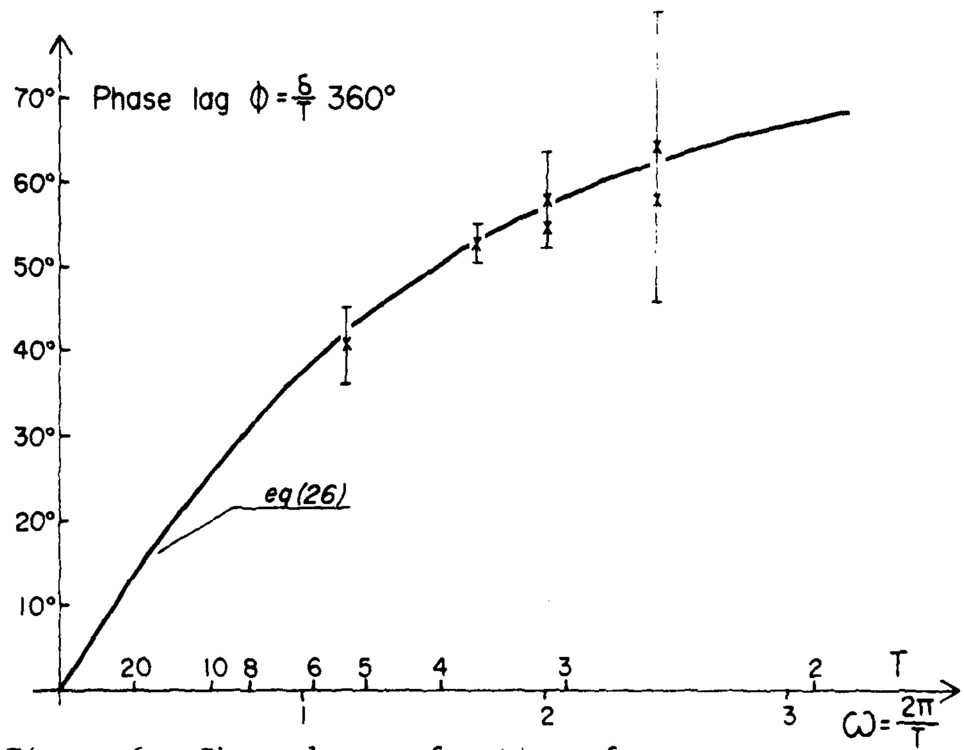

Figure 6: Phase lag as function of ω.

In the complex formalism a simple harmonic velocity is represented by an exponential:

$$u(t) = Ue^{i\omega t} = U(\cos \omega t + i \sin \omega t) \qquad (20)$$

of which only the real part $U \cos \omega t$ is given physical meaning.

For a flow meter with gain G and phase lag ϕ, the output related to u(t) is then

$$v(t) = GU\{\cos(\omega t-\phi) + i \sin(\omega t-\phi)\} \qquad (21)$$

$$v(t) = GUe^{i(\omega t-\phi)} \qquad (22)$$

$$v(t) = Ge^{-i\phi} u(t) \qquad (23)$$

The factor $Ge^{-i\phi} = F(\omega)$ is called the <u>frequency response function</u>.

The solid lines in figures 5 and 6 both correspond to a frequency response function given by

$$F(\omega) = \frac{1}{1 + i.77\omega} \qquad (24)$$

which is seen to fit the experimental data very well. From equation (24) the gain and phase lag can be determined

$$G = |F(\omega)| = \frac{1}{\sqrt{1 + (.77\omega)^2}} \qquad (25)$$

$$\phi = -\arg\{F(\omega)\} = \tan^{-1}(.77\omega) \qquad (26)$$

The position of $F(\omega)$, as given by equation (24), in the complex plane is shown in figure 7.

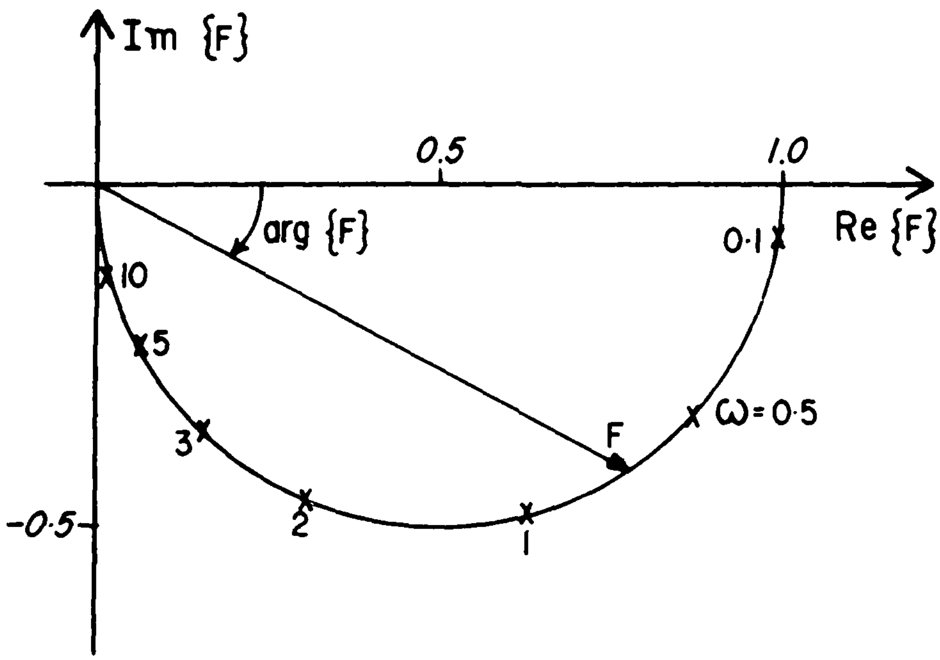

Figure 7: The frequency response function $F(\omega)$ describes a semi circle as ω goes from zero to infinity.

Correction of Spectra

The analytical expressions (25) and (26) can be used to correct energy spectra, obtained with these flow meters.

If the observed value at ω is $S^1(\omega)$, then from (25) we see that the corrected value is

$$S(\omega) = G^{-2}S^1 = \{1 + (.77\omega)^2\}S^1 \qquad (27)$$

and if the observed phase angle is $\psi^1(\omega)$, the corrected value is

$$\psi(\omega) = \psi^1(\omega) + \tan^{-1}(.77\omega) \qquad (28)$$

Direct correction of time series

Instead of correcting the spectrum one can correct the time series directly. But first we must find the equivalent of equation (24) in time domain.

For each fourier component u_ω of the input velocity and the corresponding output v_ω we have

$$v_\omega = F(\omega)\, u_\omega \tag{29}$$

and applying equation (24) this gives

$$v_\omega + .77 i\omega v_\omega = u_\omega \tag{30}$$

Now, as v_ω is a simple harmonic we have $i\omega v_\omega = \frac{dv_\omega}{dt}$ and thus

$$v_\omega + .77 \frac{dv_\omega}{dt} = u_\omega \tag{31}$$

Since this equation holds for every fourier component, and differentiation is a linear operation, it holds for the total velocity. So for any input $u(t)$ and output $v(t)$ we have

$$v + .77 \frac{dv}{dt} = u \tag{32}$$

This leads to extremely simple correction formulae for discretely measured velocities $v(t_m)$. If we put

$$v(t_{m+\frac{1}{2}}) = \tfrac{1}{2}\{v(t_m) + v(t_{m+1})\} \tag{33}$$

and

$$\left.\frac{dv}{dt}\right|_{t_{m+\frac{1}{2}}} = \frac{v(t_{m+1}) - v(t_m)}{\Delta t} \tag{34}$$

where Δt is the time step length, we get

$$u(t_{m+\frac{1}{2}}) = (0.5 + \frac{.77}{\Delta t})v_{m+1} + (0.5 - \frac{.77}{\Delta t})v_m \qquad (35)$$

and with a step length of one second:

$$u(t_{m+\frac{1}{2}}) = 1.27v(t_{m+1}) - .27v(t_m) \qquad (36)$$

The meaning of (35) is shown in figure 8 in the case of a sharp crested saw tooth input

$$u(t) = 1 - \frac{2t}{10}, \quad 0 < t < 10 \qquad (37)$$

extended periodically beyond the points $t = 0$ and $t = 10$.

The sampled values $v(t_m)$ will always be taken from the curve "$v(t)$" no matter what the sampling interval is. This curve corresponds to equation (38).

However the corrected values $u_1(t)$ and $u_{\frac{1}{2}}(t)$ give better and better approximations to $u(t)$ with decreasing sampling interval. This is because (34) is a better estimate of the derivative $\frac{dv}{dt}$ for small step lengths, Δt.

In general the multiplication

$$v_\omega = F(\omega)\ u_\omega \qquad (29)$$

in the frequency domain corresponds to a convolution in the time domain.

We find this convolution by solving (32) with respect to v,

$$v(t) = \int_{-\infty}^{t} u(\tau)\frac{\exp\{-(t-\tau)/.77\}}{.77}\,d\tau \qquad (38)$$

(compare with Jenkins and Watts (1968): Spectral Analysis and its Applications, p.35)

This shows that the impulse response function of the system is

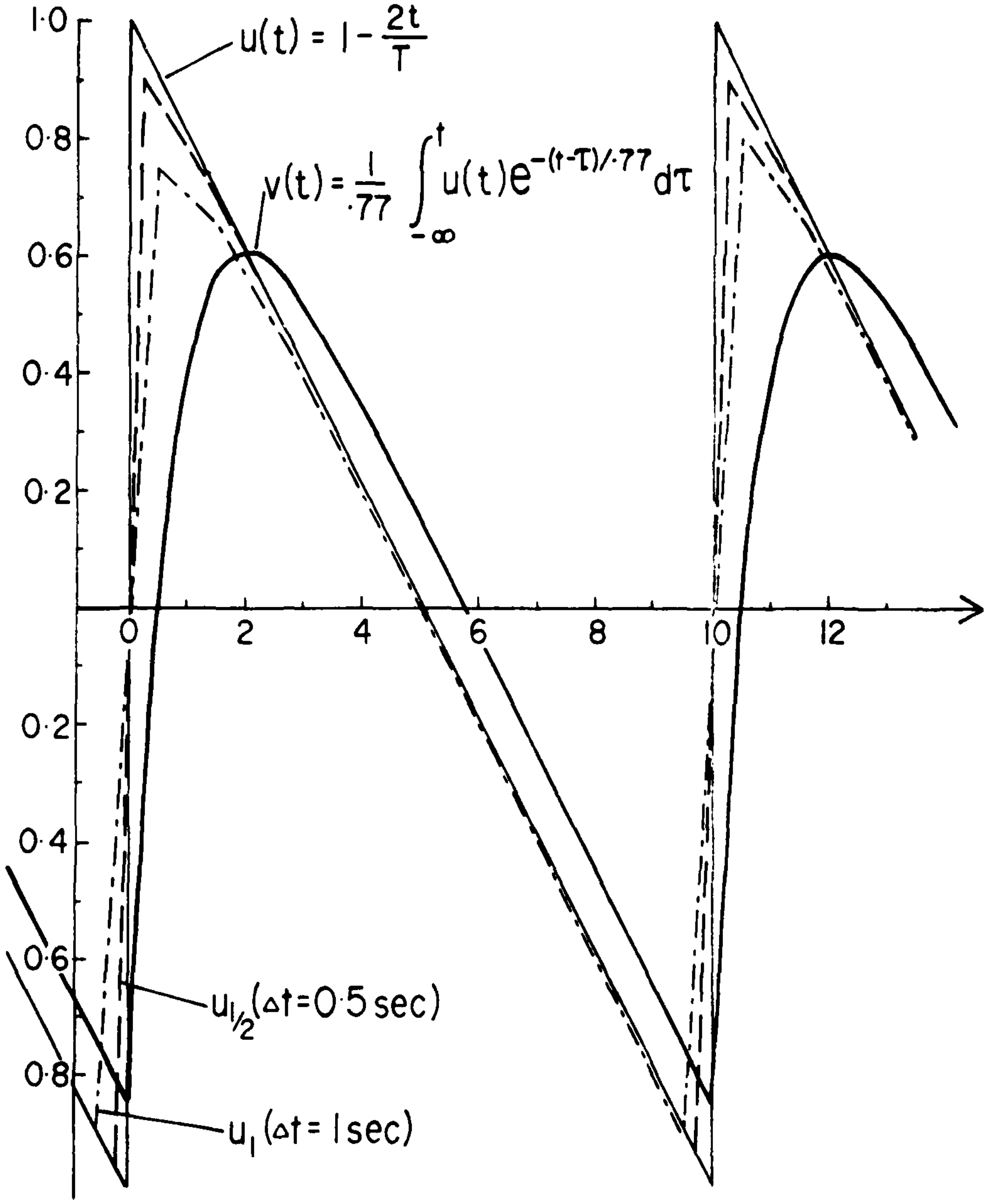

Figure 8: Sampled and corrected velocities in the case of a saw tooth bore of 10 seconds period.

$$h(x) = \begin{cases} \frac{1}{.77}\exp\{-(t-\tau)/.77\} & \text{for } \tau \leq t \\ 0 & \text{for } \tau > t \end{cases} \qquad (39)$$

That is, the flow meter remembers velocities in the past, (at $t = \tau$), to an extent that decays exponentially with the time interval $(t - \tau)$.

Tests with off axial flow.

A series of tests were carried out with constant period, T = 3.6 sec, but with the flow meter placed at different angles to the flow.

Gain values were obtained as the ration between actual V-values and the corresponding smoothed U values, $\hat{U}$. See figure 9.

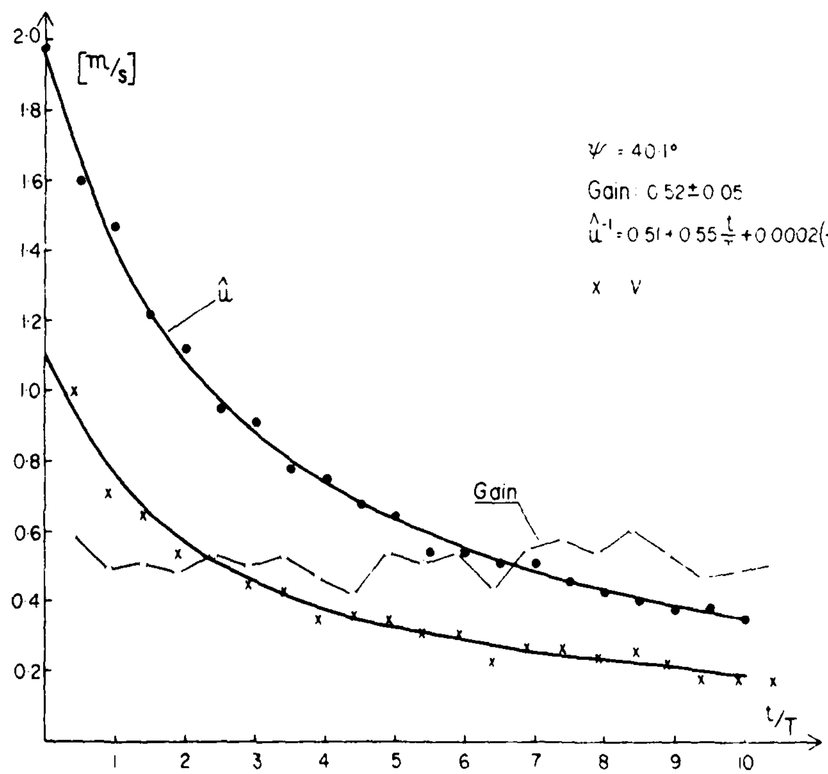

Figure 9: Velocity and gain values for $\psi = 40.1^\circ$. Even at this angle the gain has only dropped to .52 from the on-axis-value .56.

Ideally the gain at the angle ψ should be

$$g(\psi) \quad = \quad G \cos \psi \tag{40}$$

where G is the on-axis-gain, given by (25). But the tests showed that the gain is nearly independent of ψ for $\psi < 40^\circ$ and that even at $\psi \simeq 90^\circ$ there is a periodic flow through the flow meter corresponding to a gain of .10 - .15.

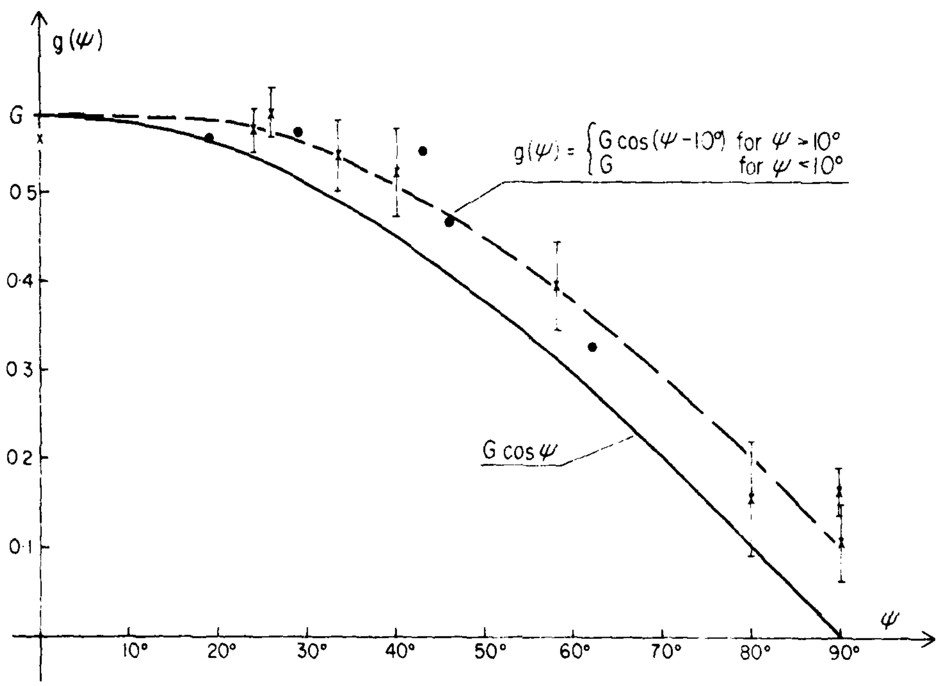

Figure 10: Off-axis-gain values g (ψ) compared to the ideal value G cos ψ.

We may approximate $g(\omega)$ by

$$g(\psi) \quad = \quad \begin{cases} G \cos (\psi - 10^\circ) & \text{for } \psi > 10^\circ \\ G & \text{for } \psi \leq 10^\circ \end{cases} \tag{41}$$

See figure 10.

Then the effect on measurements are as shown in figure 11.

It is seen that the observed velocity $\vec{v}/G$ is larger than the real velocity $\vec{u}$, and also that $\vec{v}$ lies closer to the 45° line than $\vec{u}$.

Under the assumption that $g(\psi)$ is given by (41) we can correct for this effect in the following way.

The measured components v_x and v_y are given by

$$|v_x| = |\vec{u}| \; G \cos (|\beta| - 10) \tag{42}$$

$$|v_y| = |\vec{u}| \; G \cos (90 - |\beta| - 10) \tag{43}$$

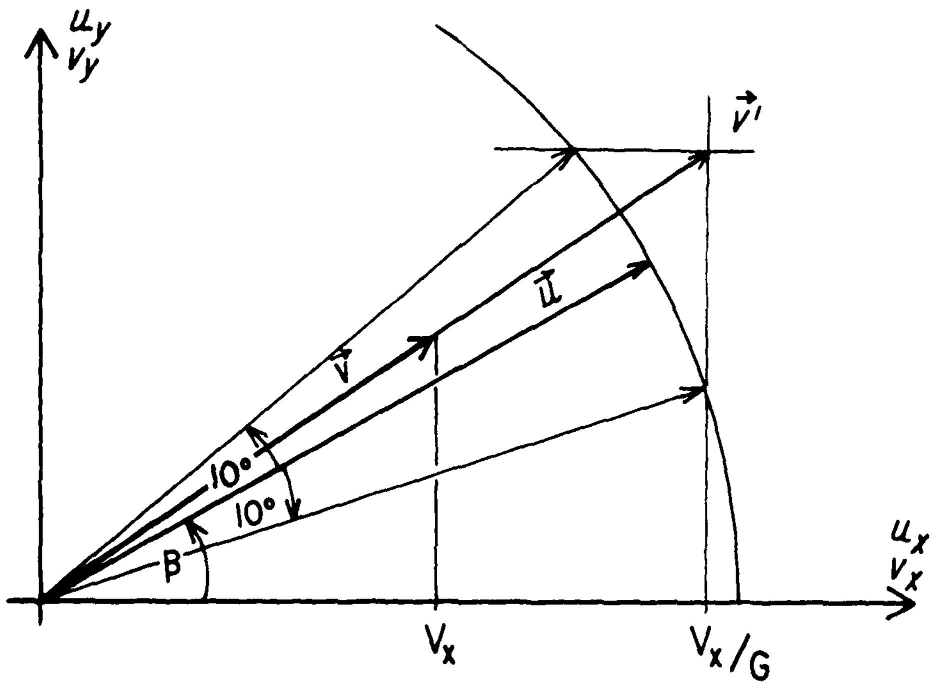

Figure 11: Real and measured velocities if $g(\psi)$ is given by equation (41).

Solving for $|\beta|$ we get:

$$|\beta| = \tan^{-1} \frac{|v_y/v_x| \cos 10^\circ - \cos 80^\circ}{\sin 80^\circ - |v_y/v_x| \sin 10^\circ} \tag{44}$$

$$\beta = \begin{cases} |\beta| & \text{for } v_x > 0 \text{ and } v_y > 0 \\ -|\beta| & \text{for } v_x > 0 \text{ and } v_y < 0 \\ -|\beta| + 180^\circ & \text{for } v_x < 0 \text{ and } v_y > 0 \\ |\beta| + 180^\circ & \text{for } v_x < 0 \text{ and } v_y < 0 \end{cases} \tag{45}$$

When β is known, $|\vec{u}|$ is readily found from (42) or (43) with G given by (25).

The formulae (44) and (45) are only valid for

$$0.1 < |v_y/v_x| < 10 \tag{46}$$

Outside this range β is undetermined. We only know that

$$\begin{aligned} |u| &\simeq v_x/G \text{ and } |\beta| < 10^\circ \text{ for } |v_y/v_x| < .1 \\ |u| &\simeq v_y/G \text{ and } |\beta-90^\circ| < 10^\circ \text{ for } |v_y/v_x| > 10 \end{aligned} \tag{47}$$

Variability between Different Flow Meters

Variation of frequency response between flow meters was examined using the pendulum for a single Θ_o and ω (19^o and $2\pi/5.5$ rad/sec respectively). Only flows parallel to the axis of sensors were used.

Tests were made for : (1) variation in experimental replication, (2) variation among all flow meters with a single control box, (3) variation due to initial swing direction, and (4) variation among control boxes for a single sensor.

For each set of tests, the ratio between peak ranges of flow meter output, V_i and P_i was measured for the 1st - 2nd and 15th - 16th peaks in the series ($i = 1$ and $i = 15$ respectively). Since the system is linear, these ratios are both related to the gain by

$$G = kV_i/P_i$$

where k is a constant of proportionality. Therefore, it also provides an estimate of the frequency response through equation 25.

Voltages P_1 and P_{15} correspond to real water velocity amplitudes of approximately 2.0 m/s and 0.4 m/s respectively. Flow meter output variability was characterised by the coefficient of variability

$$C_i = \frac{[\mathrm{Var}\ \{V_i/P_i\}]^{\frac{1}{2}}}{\overline{V_i/P_i}}$$

for each set of tests, in order to stress the significance of the variability relative to output magnitudes.

Test Procedure Variability

Outputs were recorded on strip chart (Rikadenki Model KA-42H). The .5 mm limit of reading for measurements taken from these records resulted in coefficients of variability of .3% for $i = 1$ and 1.2% for $i = 15$.

Experimental replicability showed variabilities of $C_1 = .6\%$ and $C_{15} = 2.7\%$. Assuming independence between variances resulting from measurements taken from the chart record and that for the test apparatus, the total variability inherent in the test procedure is therefore $C_1 = .5\%$ and $C_{15} = 2.4\%$.

Variability between flow meters for a single box was found to be C_1 = 1.7% and C_{15} = 5.3%. More than half of this is accounted for by experimental variability. The contribution due to initial swing direction was found by averaging over all sensors the variance of P_i/V_i for each pair of swing variability ($\bar{C}_1$ = .4% and $\bar{C}_{15}$ = .5%) is less than that attributable to the test procedure.

Variability between control boxes for a single sensor showed similar results (C_1 = 2.8% and C_{15} = 3.9%).

Total Variability between flow meter systems resulting from both sensor and control box variances can be concluded to be C_1 = 3.2% and C_{15} = 5.6%, taking into account variance introduced due to the experimental procedure.

As a rule of thumb therefore total variability between flow meter systems may be assumed to be 5% of velocity amplitude.

Version 1 Control Box Time Constant

There are two versions of the control boxes currently in use. Tests reported above concern 'Version 2' control boxes which are more commonly in use. Version 1 control boxes are similar in concept to the Version 2 boxes. However, these boxes do not incorporate a 'fast' filter option as with the later model. The minimum filter option is specified as 1 second.

Since the system is linear the gains of both the Version 1 and Version 2 systems (denoted as G_1 and G_2 respectively) can be determined by

$$G_1 = k(V_i/P_i)_1$$

$$G_2 = k(V_i/P_i)_2$$

as described above, so that

$$G_1 = G_2 \, (V_i/P_i)_1 \, / (V_i/P_i)_2$$

From equation 25, for $\omega = 2\pi/5.5$, G_2 = 0.75, and using test means for V_i/P_i it is found that

$$G_1 = .58 \quad , i = 1$$

$$G_1 = .60 \quad , \quad i = 15$$

Averaging G_1, substituting into the general form of (25)

$$G = \{1 + (T\omega)^2\}^{\frac{1}{2}}$$

and solving for the time constant yields T = 1.21 for the earlier 'Version 1' control boxes. Accuracy of T from the empirical determinations is ±2.3%.

Therefore, when considering output from 'Version 1' control boxes T = 1.21 should be substituted for the constant .77 wherever it occurs in this report.

SECTION 2

CALIBRATION OF STRAIN-GAGE PRESSURE TRANSDUCERS

Abstract

The purpose of the experiments described in this section was to calibrate the Coastal Studies Unit's pressure transducers. Tests were made for response time, gain for hydrostatic pressures, accuracy of the hydrostatic pressure offset facility (see appendix), and the variation between transducer-systems.

Correction procedures are also described for obtaining wave height and water surface elevation obtained from pressure records.

Experimental Setup

To test response time, the transducer orifice was sealed within a small, waterfilled test reservoir (figure 12). The reservoir was connected via a valve to two water filled plastic tubes of 5 mm internal diameter. The water levels in the tubes were placed at respective heights h_1 and h_2 relative to the transducer.

The pressure p in the test reservoir in general is

$$p = \rho g h \tag{2.1}$$

where ρ is water density and g is gravitational acceleration. Turning the valve therefore provides an instantaneous pressure change, Δp of

$$\Delta p = |\rho g(h_1 - h_2)| \tag{2.2}$$

Application of this pressure pulse provided the basis for the response time test.

Hydrostatic pressure gain was tested by moving the long pressure-head tube through h whilst connected to the test reservoir. The gain, G was then determined as the ratio

$$G = H/h \tag{2.3}$$

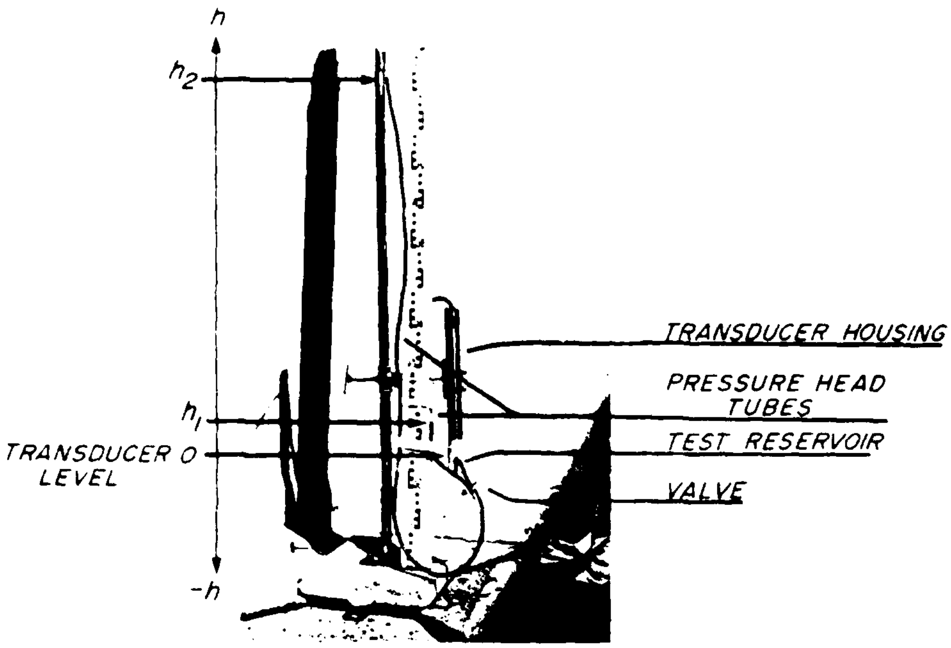

Figure 12: Experimental set up. The transducer orifice is at the lower end of the housing (at h = 0) and contained within the water-filled test reservoir. Water in the pressure-head tubes is dyed with $KMnO_4$ for visualisation.

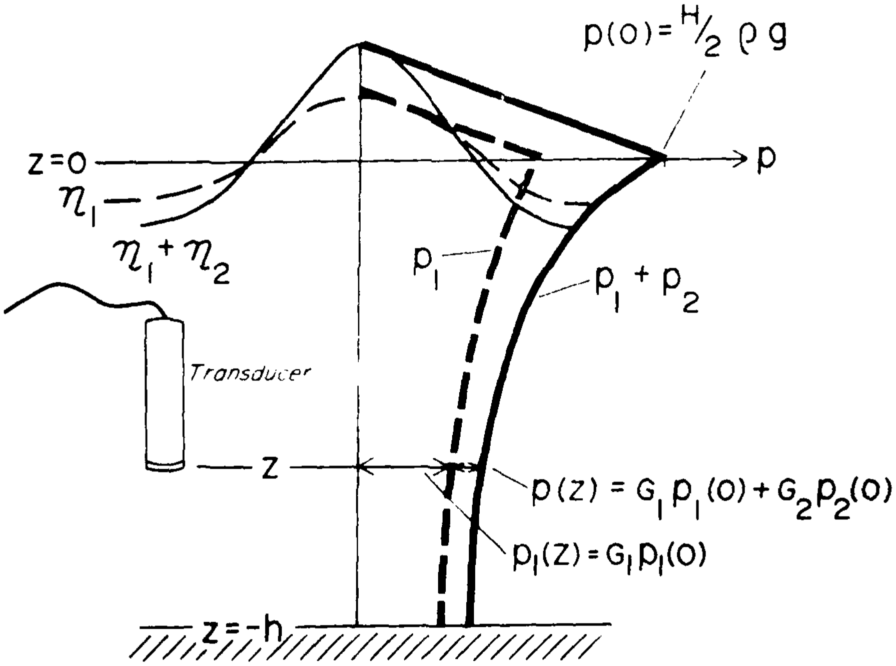

Figure 13: Combined component attenuation with depth. The schematic distributions are for a primary wave (kh) and its harmonic (2kh). In each case, rates of attenuation correspond to that of a free wave with the same kh. Pressure grows linearly from the surface down to z = 0 and then decreases hyperbolically downwards.

where

$$H = \hat{p}/\rho g \tag{2.4}$$

is the height measured by the transducer system in response to a given applied pressure, ρgh.

The pressure offset facility was tested using the same procedure.

Results

Response times were smaller than that of the chart record pen (Rikadenki Model KA-42H) used to measure it. Response time is therefore considered to be effectively zero.

Gain was found to be constant for the pressure head ranges tested (h = .5, 1.0, 5 m), with an average coefficient of variation of .8% for each sensor and 2.4% between different systems. The average gain was .952.

Frequency Response Function As explained for equation (23) the general form of the frequency response function is

$$F(\omega) = Ge^{-i\phi}$$

Since the time lag ϕ was found to be zero, the frequency response function of the transducer system can be expressed as

$$F(\omega) = Ge^{o} = G$$

Offset Though scaled in units of depth, the relationship between offset and real piezometric head was very poor, and highly variable from one transducer system to another.

General Conclusion The transducer systems have a constant gain factor of .95. In view of the zero response time this gain should hold for all frequencies in and lower than the gravity-wave spectrum.

Offset values are meaningless.

No account was made in these tests for the effects of the nonlinear Bernoulli term $\frac{1}{2}\rho(\vec{u})^2$. Nor are these effects corrected in usual analysis procedures. Under field conditions errors due to these effects may exceed 10% (Thornton, 1980), though it would appear that they are less than 20% (Guza and Thornton, 1980).

Wave height from pressure record

The primary purpose of the pressure transducer system is to measure wave heights and water surface time series. Output and control box settings are referred to in units of height, η. In reality this is merely an electronic sealing of the constant ρg so that

$$\eta = p/\rho g \qquad (2.5)$$

where η is the surface elevation.

However, in its application the pressure transducer is deployed at some fixed point below the mean surface ($z = 0$) and above the bed ($z = -h$). Because of this, the system has an inherent gain, G when used as a wave height sensor, or a water surface sensor in the presence of waves. This gain results from the attenuation of excess pressure with depth. Thus for a surface elevation $p/\rho g$ measured at a point z/h below the surface

$$p(z/h)/\rho g = \eta G(z/h) \qquad (2.6)$$

For a sine wave with wave number, k the gain may be found by

$$G(z/h) = \frac{\cosh k(z+h)}{\cosh kh} \qquad (2.7)$$

Figure 13 shows schematically the attenuation of the first two harmonic components of a nonlinear wave. The composite pressure distributions are shown, but the attenuation rates are the same for free waves of the same respective kh.

It should also be noted that for either free waves or harmonic components of sufficiently large kh the excess pressure will not be sensible at the depth of the transducer.

Optimising Sensor Deployment

Figure 14 shows variation of gain with kh at each quarter depth increment. It is clear that best resolution for waves with larger kh is achieved by deploying pressure senors as close to the mean water surface as possible. It is also evident that the resolution improves faster approaching the surface.

Correction of water surface spectra

When the pressure record is used to determine

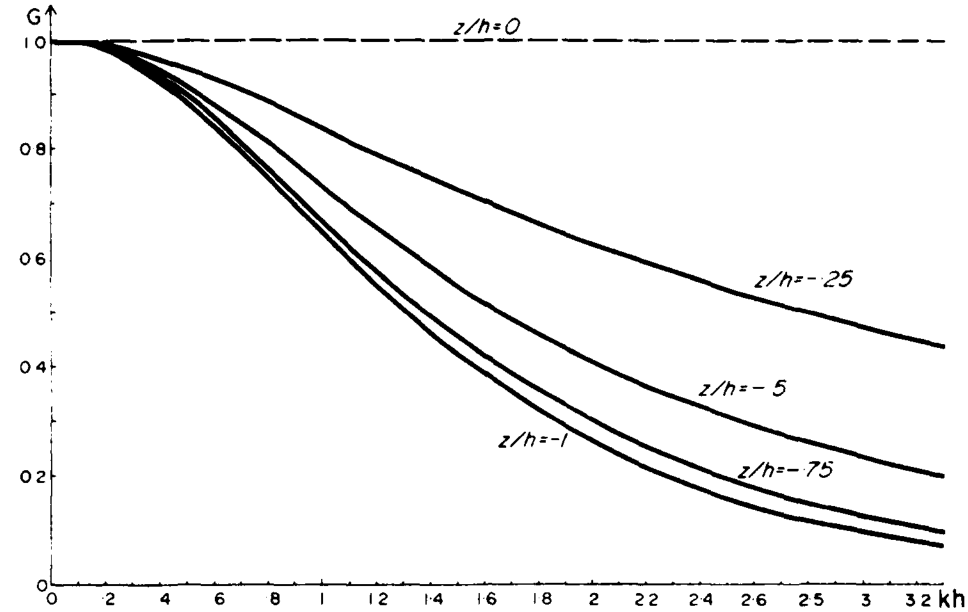

Figure 14: Variation with kh of excess-pressure gain, G due to depth according to linear theory (equ. 2.7) for quarter depth increments.

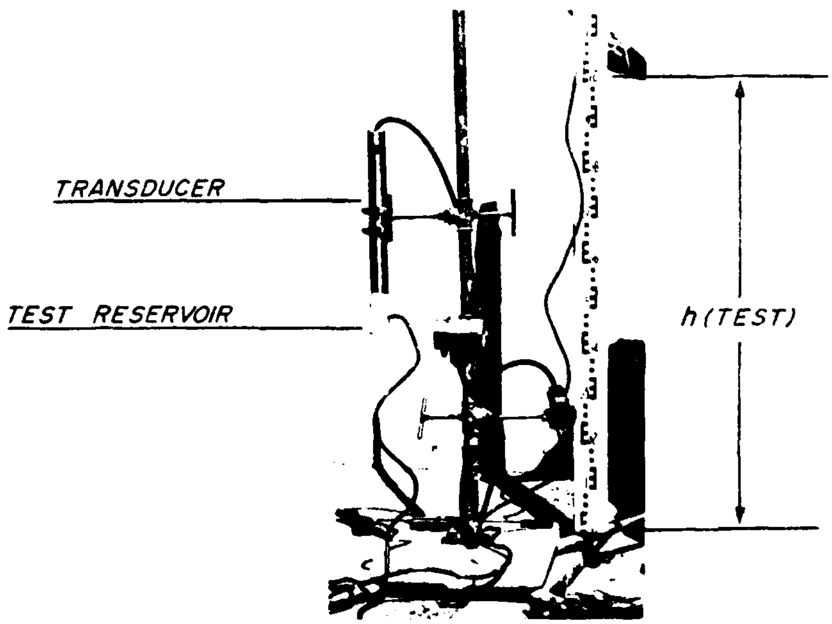

Figure 15: Field calibration apparatus. The transducer orifice is sealed within the sea water filled test reservoir. The plastic hose (5 mm i.d.) enters the test reservoir to provide a piezometric head fixed at known elevations whilst output is recorded. (The water in the tube is dyed for visual presentation).

the water-surface spectrum, the spectrum can be corrected using equation (2.7). Thus if the measured spectral estimate at ω is $\hat{S}(\omega)$ then the corrected estimate for the water surface is

$$S(\omega) = G^{-2}(\omega)\hat{S}(\omega) \tag{2.8}$$

where kh in (2.7) must be determined from the local ω by usual methods using linear theory.

Correction of water surface time series

This is not possible directly for irregular waves. However, it can be achieved indirectly by reconstitution of the time series from the corrected spectrum.

Field determination of z/h

The accuracy of the correction procedures depends upon the accuracy with which z/h is determined. In the field h can be determined by obtaining insitu output segments at the beginning and end of pressure records using a long (100 second) filter setting on control boxes. These are compared with test output when sensors are removed from the water.

The onshore test output is obtained using the calibration apparatus shown in Figure 15. The height of the water in the tube above the mounting base corresponds directly to the water depth, h.

Acknowledgements

This research has been supported by the U.S. Office of Naval Research, Task NR 388-157 and the Australian Research Grants Committee. The instruments were obtained through support from the Australian Research Grants Committee and were developed by Hales and Rogers Pty. Ltd.

References

Guza, R.T. and Thornton, E.B., 1980, Local and shoaled comparisons of sea surface elevations, pressures and velocities, J. Geophys. Res., v. 85, C3, pp. 1524 - 1530.

Jenkins, G.M. and Watts, D.G., 1968, Spectral analysis and its applications, Holden-Day, 523 pp.

Thornton, E.B., Breaking Wave Processes, Report on U.S. Office of Naval Research contract no. 388-114.

APPENDIX

Description of Field Data Acquisition System:

"Field Monitoring and Analysis
of Beach and Nearshore Hydrodynamics"

by M.P. Bradshaw, J. Chappell,
R.S. Hales and L.D. Wright

Reprinted from the
Proceedings of the 4th Australian
Coastal & Ocean Engineering Conference,
Adelaide, 1979, pp 171-175

Fourth Australian Conference
on Coastal & Ocean Engineering
Adelaide, 8-10 November 1978

Field Monitoring and Analysis of Beach and Nearshore Hydrodynamics

M. P. BRADSHAW
Senior Research Assistant, Coastal Studies Unit, Department of Geography, The University of Sydney

J. CHAPPELL
Reader, Department of Geography, School of General Studies, The Australian National University

R. S. HALES
Director, Hales & Rogers Pty. Ltd

and

L. D. WRIGHT
Associate Professor, Coastal Studies Unit, Department of Geography, The University of Sydney

SUMMARY An instrumentation system employing pressure sensitive transducers, bi-directional flow meters, and a mobile mini-computer and data logger has been developed for high resolution monitoring of wave and current activity in the nearshore zone. Transducers are used to measure incident wave characteristics, rates of energy dissipation, radiation stress gradients and low frequency oscillations of surf zone water level. Low threshold, low inertia miniature flow meters are used to observe nearshore circulation patterns, oscillatory bed velocities and swash-backwash velocities. A mobile TEKTRONIX 4051 mini-computer and multiplexing system enables analogue signals from up to 16 sensors to be stored in a digital form on magnetic tape. On-site processing of logged data can be carried out to facilitate real time analysis and interactive experimental control. In addition, data can be recorded and displayed in a visual form on multi-channel chart recorders. On return to the laboratory, the mini computer can be immediately interfaced to a large computer to provide full data analysis and storage facilities. The system has been used in a recent study of New South Wales beaches to observe inshore wave and current behaviour and associated resonant phenomena.

1 INTRODUCTION

In 1976 a long-term project was initiated at Sydney University to investigate the physical processes responsible for the characteristic patterns of sediment transport, deposition and erosion on the southern and central New South Wales coast and to identify the causal links between hydrodynamic behaviour and morphologic response. The frontier nature of this project demanded that considerable time be spent in the initial phase developing a comprehensive surf zone monitoring system. Continual refinement of our early techniques and instrumentation has led to a sophisticated and versatile system capable of high resolution monitoring of wave and current activity in the surf-zone, the nearshore zone and on the inner continental shelf.

Monitoring of inshore and beach face processes have in the past been carried out by ourselves and others using few sensors (rarely more than six) and recording data in a graphic form on strip charts. (Kirk, 1971; Sonu et al., 1973; Waddell, 1973). Several limitations inherent in this technique are:
(i) There is a low limit to the number of instruments that can be monitored simultaneously; few chart recorders have more than 6 channels.
(ii) The recorded data are not in a form that can be immediately analysed by a digital computer; charts must be manually digitized before analyses can be carried out.
(iii) Because of the necessity to digitize records, there is a low limit to the length of records that can be collected.

To overcome these problems, we required a system that would:
(i) monitor at least 12 channels of input information simultaneously.
(ii) store large data sets in a ditigal form ready for processing by computer.
(iii) facilitate a limited amount of on-site analysis in order to achieve a degree of interactive experimental control.

2 INSTRUMENTATION

2.1 Wave Measurement

Nearshore and inshore water surface oscillations are measured by up to eight pressure transducers deployed either singly or in an array. The applicability of these devices for the monitoring of ocean waves has been discussed by many, especially Williams (1969), Esteva and Harris (1970), and Ribe and Russin (1974). They were chosen in this instance for their ease of installation in the surf zone and for their reliability and ruggedness. Water surface "piercing" detectors such as parallel resistance wire gauges, capacitance gauges, and step resistance gauges have all proved difficult to install in the surf zone even under moderate wave energy conditions. In addition, they are susceptible to fouling by seaweed and to wave splash which can give rise to spurious signals, especially in the case of the resistance type gauges. Problems associated with wave-pressure attenuation due to depth are not encountered in shallow water surf zone applications and records can be corrected numerically when measurements are required in deeper water (Esteva and Harris, 1970; Kim and Simons, 1974).

The transducers used are Schaevitz Model P 741 with a range of 0-5 bars absolute, combined non-linearity and hysteresis of 0.5% full range output and a sensitivity capable of resolving changes in water level of less than 1 cm. These characteristics together with high stability against drift make them ideally suited for the measurement of low frequency, very low amplitude oscillations (e.g., beach water table) as well as the high frequency oscillations observed in the surf zone.

Each transducer is housed together with an integrated amplifier in a water-tight stainless steel cylinder measuring 25 cm in length and 4 cm OD. Connection to the shore-based power supply and control circuitry is made via 2 or 4 core cable. Three proto type transducers received power and transmitted signals over separate lines and therefore required expensive 4 core cable. In addition, the direct analogue outputs of these transducers were susceptible to attenuation due to line length and leakage. The latter is particularly a problem in the surf zone where the continual movement and flexing of cable joints can result in water penetration of even the most carefully sealed connections. Five later transducers were fitted with integrated voltage to frequency converters which modulate the power supply with a frequency proportional to pressure. The modulation is detected by shore-based control circuitry and reconverted to an analogue signal. This technique enables both power and return signals to be accommodated in 2 cores and renders return signals insensitive to line loss attenuation.

2.2 Current Measurement

Eight low inertia, bi-directional miniature flow meters are used to observe nearshore circulation patterns, oscillatory bed velocities and swash-backwash velocities (Fig.1). Similar sensors have been used by others to measure rip current velocities (Sonu, 1972), to record flow velocities in the swash zone (Sonu et al.,1974), and for general purpose monitoring of surf zone currents (Teleki et al.1976). The meter comprises a stainless steel duct (measuring 9 cm in length and 5.5 cm internal diameter) which houses a six-bladed impellor made of light-weight plastic, and suspended on jewel bearings. Threshold velocity is approximately 5 cm/sec (Sonu et al., 1974) and the meter has a cosine response to current direction (Murray, 1969), making it straightforward to determine a fluctuating two-dimensional current field by using orthogonal meters. Lightweight alloy magnets attached to the impellor activate sensitive reed switches in the barrel, the pulses from which are transmitted to shore via 2 - core cable and decoded by control modules to give a readout of current velocity and direction.

Few problems have been encountered with these current meters. They are small, rugged and easily moved into position in the surf zone. Since signals are "pulsed" there are no problems of line attenuation or undetected leakage; the presence of any leakage is immediately revealed by total loss of signal. Seaweed and gravel have, however, proved troublesome on occasions and it is sometimes necessary for personnel to enter the surf during an experiment to clear debris from the impellor. The meter will respond to wind flows immediately it becomes completely exposed to the air; a cut-off switch is currently being built to return the sensor output to zero as soon as it becomes fully exposed.

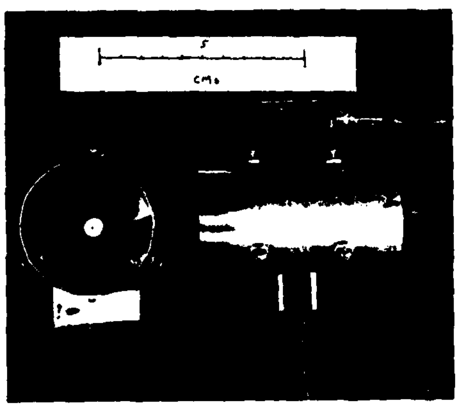

Figure 1 Ducted flow meters

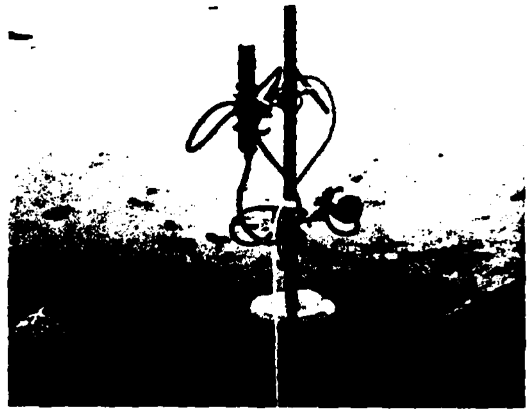

Figure 2 Instrument mounting with sensors attached

2.3 Sensor Deployment

Experimentation in the surf zone, particularly under the high energy conditions normally experienced on the New South Wales coast, presents formidable logistic problems which we have attempted to overcome with reasonable success.

Different methods of mounting and deploying instruments received considerable attention during the early stages. The mounting design which has proved most successful is constructed from threaded sections of 1½ inch galvanized pipe which connect into a central concrete base. Instruments are attached to the upright by quick release clamps. This can be done either before or after the mounting is positioned for an experiment, depending on energy conditions and the depth of the installation. Pipes one metre long extending horizontally from the center of the mount provide stability even under heavy surf. The entire structure is light and manageable enough to be installed by two men. Figure 2 shows a flow meter and pressure transducer attached to a mounting.

The transmission of signals by cable remains a major shortcoming of the system. Wave turbulence and longshore currents often result in broken cables. Lines frequently must be strung across a trough from high towers. The use of telemetry is currently being examined as a possible solution to this problem.

2.4 Signal Processing and Logging

Control circuitry for all sensors is housed in a small camper van (Fig.3) together with a mini-computer and multiplexing system and two strip chart recorders. The control modules decode flow meter and transducer signals and in addition provide:
(i) variable range settings from 0.1 to 5 metres (m/sec in the case of the flow meters).
(ii) depth offset adjustment for the transducers.
(iii) variable input filters with response periods between 0.1 and 100 seconds.

Signals are digitized and logged by a computer system comprising a TEKTRONIX 4051 mini-computer and a Hales Data Acquisition system. The former is a 16K byte machine with an extended BASIC operating system residing in a separate 32K ROM. It has an in-

Figure 3 Interior of field unit

tegrated keyboard and high resolution graphic display screen as well as two cartridge tape drives.

The Hales Data Acquisition system (DAS-1) is a combined A-to-D converter, scanner and multiplexer which accepts analogue signals from up to 16 channels. It has a resolution of 12 bits binary full scale (1 part in 4096) and an overall accuracy of 0.1%. The time base is crystal controlled with an accuracy of 0.02% and has a period adjustable from 1 millisecond to 262 seconds in 1 millisecond increments. The 16 channels can be scanned either sequentially or simultaneously at a rate set by the time base and the data fed directly to the computer via a standard IEEE-488 interface bus. Data is stored on magnetic tape cartridges each capable of holding 30,000 observations.

In addition, analogue outputs from the sensor control modules can be recorded and displayed in a visual form on two multi-channel strip chart recorders. A segment of record from three surf zone sensors is shown in Figure 4.

The TEKTRONIX 4051 was chosen, not only for its portability, ease of programming, and graphics capabilities but also because of its ability to be interfaced with larger computers, thereby serving as a terminal and data transfer station. This facility enables field data to be transferred to the University's Cyber 72 for storage and analysis immediately the mini-computer is returned to the laboratory.

3 SYSTEM APPLICATIONS

3.1 Inshore Applications

In any given surf zone, the spectrum of motion is made up of numerous progressive (dissipative) and standing (reflective) components (Huntley et al., 1977). On a steep reflective beach, oscillations at incident wave period are normally standing near the beach; however, with decreasing inshore slope and increasing surf zone turbulent viscosity, high frequency reflection is suppressed and the periods which can be standing increase through a progression of subharmonics (jT; where j = 2 or 4) to surf beat period (T_b = 80 - 150 sec) to a very low frequency seiching at periods (T = 5 - 10 mins) near the natural compartment period (Wright et al., in press, a & b). The standing oscillations can exist either as "leaky" modes in which the reflected energy is reradiated back to sea (Suhayda, 1974) or as resonant trapped edge waves.

Field studies indicate that spatial and temporal variability of beach profile response, "rhythmic" or three-dimensional beach features and their scales and intensities are all functions of the relative degrees of inshore resonance versus dissipation. At the high frequency end of the spectrum, cusp initiation can be linked to edge waves oscillating at incident frequencies on reflective beaches (Wright et al., 1977). As turbulent viscosity increases the concomitant increase in resonant period is accompanied by increasing scale of morphological features (e.g., rip spacing and associated rhythmic topography) and increasing intensity of circulation (e.g., rip velocity). A major part of our study has been concerned with investigating the interrelationships between various types of inshore topography and their associated scales of resonance (Wright et al., in press, a & b). To this end we have focused on a range of characteristic beach types using experimental configurations similar to that shown in Figure 5. Pressure transducers are used to obtain data on both the input wave characteristics and the water surface oscillations in the surf zone. Flow meters monitor currents in both the shore normal and the shore parallel direction. Both types of sensors can be arranged to gather simultaneous information on the spatial variations in surf zone oscillations either normal to or parallel to the shoreline. In addition, the relationship between water surface oscillations and current flows at particular points can be studied by monitoring flow meters and a pressure transducer together as shown in Figure 2.

Analysis of wave and current records is undertaken on two scales:

(i) Field software has been written for the TEKTRONIX 4051 to enable computation of power spectra for up to 1200 points of single series data. In addition, data logging software provides for continuous graphic display of running means for one channel of current data and periodic display of wave data. Current statistics (bi-directional means, standard deviations, skewness, max and min velocities) can be computed for an unlimited number of observations.

The ability to carry out preliminary processing in the field allows for some degree of interactive control over experiments by providing an indication of the scale and intensity of processes operative at the site.

(ii) On return to the laboratory, full spectral and cross-spectral analysis can be carried out on multiple series using the Biomed BMD02T Time Series Analysis Program. Computation of cross-spectral phase

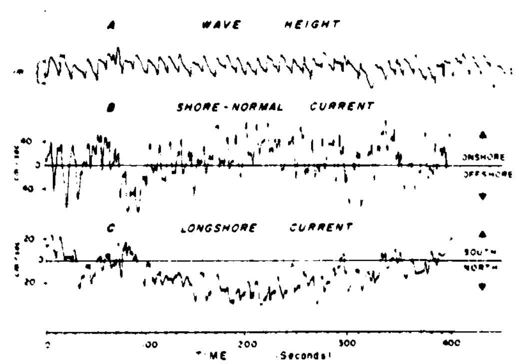

Figure 4 Sample time series of surf-zone pressure sensor and current meters

and coherence relationships for water surface elevation and current records are needed to substantiate the existence of resonance; in progressive waves horizontal velocities and surface elevations are in phase whereas in standing waves surface elevation lags flow by $\pi/2$ at positions other than nodes or antinodes.

Figure 6 shows results of spectra obtained from instruments located in a longshore trough bounded on its seaward edge by a well developed bar, 75 metres from the beach face. The wave height spectrum shows a primary peak centred at 0.093 Hz (10.8 secs), a well developed harmonic peak at 0.18 Hz and a high, very sharp infragravity peak near 0.02 Hz (50 secs). From the same position, the shore normal current spectrum shows a dominant peak at incident wave frequency (0.094 Hz) and a strong second peak in the region of 0.02 - 0.025 Hz (i.e., 4T). Examination of the coherence and phase relationship for these two sensors shows moderate coherence and a $\pi/2$ phase relationship at the strong 4T subharmonic, thus indicating the existence of resonance at this frequency.

In addition to the principle tasks just described, the field based mini-computer has also proved useful as a surveying tool by:
(i) enabling the storage and overlay plotting of beach profile data and;
(ii) plotting, in real time, the movement of plastic seabed drifters released in the surf zone. This technique involves the tracking by dual theodolites of snorkelers swimming above the slightly negatively buoyant sea bed drifters. We have found that it provides valuable information on the movement of inshore currents (*especially* rips).

3.2 Offshore Applications

The portability of the data acquisition system has enabled it to be used successfully as a shipboard monitor of offshore wave conditions and bottom currents. Preliminary experiments have been carried out in embayments on New South Wales coast to study wave induced bottom current behaviour and to investigate the possible role of other processes such as bay seiching. In these experiments pairs of flow meters were diver mounted just above the bottom at depths slightly over 20 m. and data was logged continuously for periods of up to 6 hours and over full tidal cycles. The only limitation of this method of collecting offshore data is that imposed by weather conditions which would preclude any experimentation during periods of heavy seas.

4 CONCLUSIONS

Field measurement of waves and instantaneous currents in high energy surf zones is a logistically difficult task and it is largely for this reason that direct observation under real world circumstances have previously been limited. Many of the problems of surf-zone instrument installation have been overcome with the development of the simple and rapid deployment techniques described. The real-time data acquisition/processing system enables large quantities of field data to be collected and analysed efficiently, with the minimum amount of intermediate laboratory processing. Difficulties remain associated with monitoring surf zone and nearshore processes under breakers greater than 3 m in height, owing to stress on the electrical cables crossing the surf zone and to hazards to the field crew working in the surf zone. A telemetry system is being developed to obviate the need for transmission of sensor signals over long cables.

Instrumentation is currently being upgraded to allow for more comprehensive experimentation on the inner shelf processes responsible for sediment movement and modification of oceanographic forces. The expanded system will include a self contained, battery powered 8 channel magnetic tape data logger and sensor signal processors housed in water tight capsules which are attached to bottom mounted tripods by divers. Flow meters, pressure transducers and other sensors (up to a total of 8) will be interfaced to the data logger, the tapes from which will

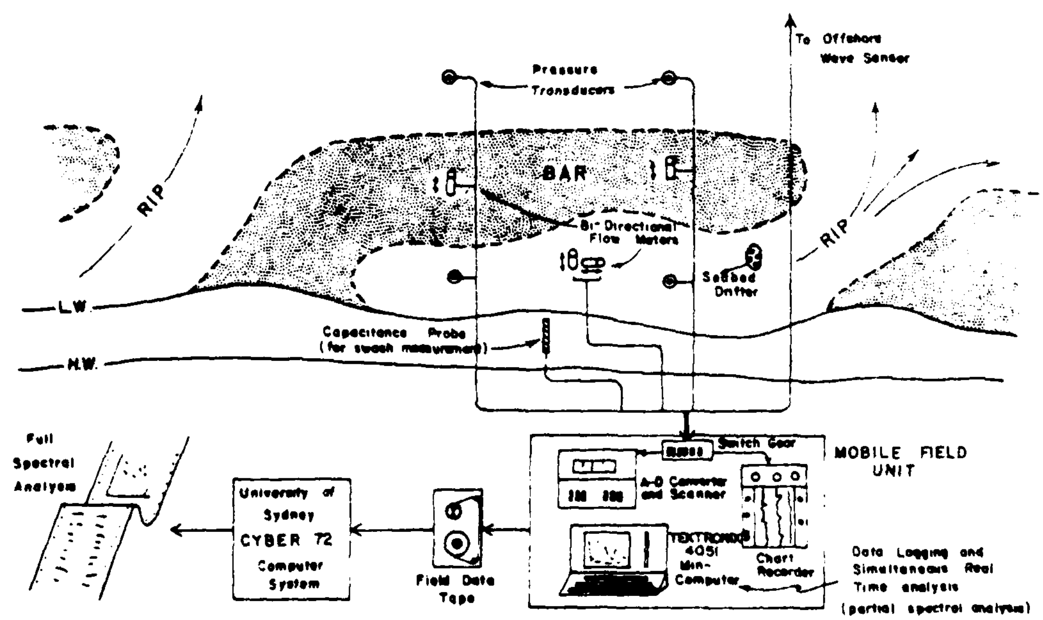

Figure 5 Typical experiment on a dissipative beach

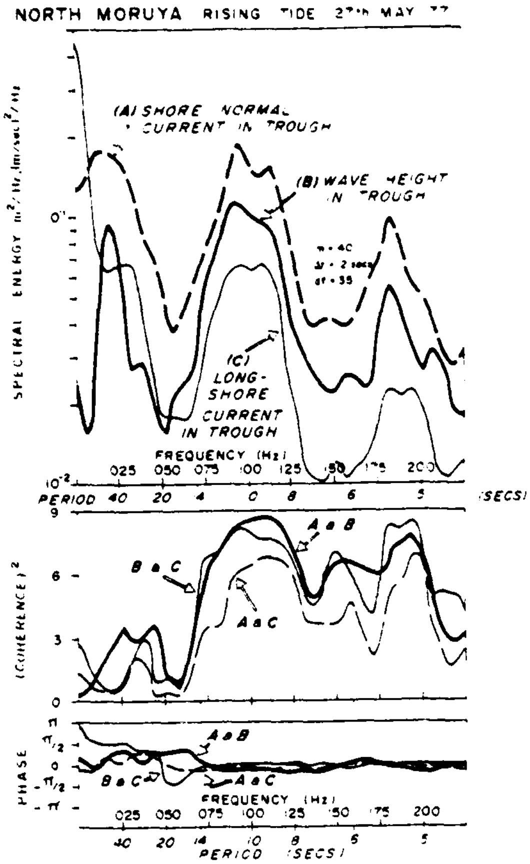

Figure 6 Sample spectra of surf-zone records

be compatible with the existing TEKTRONIX computer system. The under-water system will permit continuous or blocked samples to be taken over periods ranging from 24 hours to 1 month, depending on the sample interval.

5 ACKNOWLEDGEMENTS

The development of the system described herein and our ongoing studies of New South Wales coastal dynamics are supported by the Australian Research Grants Committee. We wish to thank P. Cowell, B.G. Thom, and A.D. Short for their assistance. Diagrams were prepared by J. Roberts and M. Rigney.

6 REFERENCES

ESTEVA, D and D.L. HARRIS (1970), Comparison of pressure and staff wave gage records. Proc. 12th Conf. Coastal Engineering, Washington, pp 101-116.

HUNTLEY, D.A., R.T. GUZA and A.J. BOWEN (1977), A universal form for shoreline run-up spectra. J. Geophys. Res., 82, pp 2577-2581.

KIM, Y.Y. and L.H. SIMONS (1974), Sea state measurements from pressure records. in Ocean Wave Measurement and Analysis, Am. Soc. Civ. Eng., New Orleans, Vol 1, pp 40-53.

KIRK, R.M. (1971), Instruments for investigating shore and nearshore processes. N.Z. Jour. Marine & Freshwater Res., 5(2).

MURRAY, S.P. (1969), Current meters in use at the Coastal Studies Institute. Louisiana State Univ - Coastal Studies Bull., No.3.

RIBE, R.L. and E.M. RUSSIN (1974), Ocean wave measuring instrumentation. in Ocean Wave Measurement and Analysis, Am. Soc. Civ. Eng., New Orleans, Vol 1, pp 396-416.

SONU, C.J. (1972), Field observations of nearshore circulation and meandering currents. J. Geophys. Res., 77(18), pp 3232-3247.

SONU, C.J., S.P. MURRAY, S.A. HSU, J.N. SUHAYDA and E. WADDELL (1973), Sea breeze and coastal processes. EOS, 55, pp 301-343.

SONU, C.J., N. PETTIGREW and R.G. FREDERICKS (1974), Measurement of swash profile and orbital motion on the beach. in Ocean Wave Measurement and Analysis, Am. Soc. Civ. Eng., New Orleans, Vol 1, pp 621-638.

SUHAYDA, J.N. (1974), Standing waves on beaches, J. Geophys. Res., 79, pp 3065-3071.

TELEKI, R.G., F.R. MUSIALOWSKI and D.A. PRINS (1976), Measurement techniques for coastal waves and currents. US Army CERC Misc. Report No. 76-11.

WADDELL, E. (1973), Dynamics of swash and implication to beach response. Louisiana State Univ. Coastal Studies Tech. Report, No. 139.

WILLIAMS, L.C. (1969), CERC wave gages. US Army CERC Tech. Memo, No. 30.

WRIGHT, L.D., B.G. THOM, P. COWELL, M. BRADSHAW and J. CHAPPELL (1977), Field observations of resonant surf and current spectra on a reflective beach and relationship to beach cusps. Search, 8(9), pp321-22.

WRIGHT, L.D., J. CHAPPELL, B.G. THOM, M.P. BRADSHAW and P. COWELL (in press), Morphodynamics of reflective and dissipative beach and inshore systems: Southeastern Australia. Marine Geology.

WRIGHT, L.D., B.G. THOM and J. CHAPPELL (in press), Morphodynamic variability of high energy beaches. Proc.16th Internat. Conf. Coastal Eng., Hamburg, 1978.

DAT
FILM